RSC Advances

PAPER

View Article Online
View Journal | View Issue

Cite this: *RSC Adv.*, 2021, **11**, 39169

Degradation kinetic study of ZIF-8 microcrystals with and without the presence of lactic acid

Sofiia A. Butonova,[a] Evgeniya V. Ikonnikova,[a] Aziza Sharsheeva,[a] Ivan Yu. Chernyshov,[a] Oleg A. Kuchur,[a] Ivan S. Mukhin,[ab] Evamarie Hey-Hawkins,[c] Alexander V. Vinogradov[a] and Maxim I. Morozov *[a]

The zeolitic imidazolate framework ZIF-8 ($Zn(mim)_2$, mim = 2-methylimidazolate) has recently been proposed as a drug delivery platform for anticancer therapy based on its capability of decomposing in acidic media. The concept presumes a targeted release of encapsulated drug molecules in the vicinity of tumor tissues that typically produce secretions with elevated acidity. Due to challenges of *in vivo* and *in vitro* examination, many studies have addressed the kinetics of ZIF-8 decomposition and subsequent drug release in phosphate buffered saline (PBS) with adjusted acidity. However, the presence of hydrogen phosphate anions $[HPO_4]^{2-}$ in PBS may also affect the stability of ZIF-8. As yet, no separate analysis has been performed comparing the dissolving capabilities of PBS and various acidification agents used for regulating pH. Here, we provide a systematic study addressing the effects of phosphate anions with and without lactic acid on the degradation rate of ZIF-8 microcrystals. Lactic acid has been chosen as an experimental acidification agent, since it is particularly secreted by tumor cells. Interestingly, the effect of a lactic acid solution with pH 5.0 on ZIF-8 degradation is shown to be weaker compared to a PBS solution with pH 7.4. However, as an additive, lactic acid is able to enhance the decomposition efficacy of other solutions by 10 to 40 percent at the initial stage, depending on the presence of other ions. Additionally, we report mild toxicity of ZIF-8 and its decomposition products, as examined on HDF and A549 cell lines.

Received 22nd September 2021
Accepted 3rd December 2021

DOI: 10.1039/d1ra07089d

rsc.li/rsc-advances

Introduction

Metal–organic frameworks (MOFs) are a class of engineered materials suitable for encapsulation of drug molecules, owing to their chemical and structural flexibility.[1] The structural diversity and functional variety of MOFs are based on a combination of metal ions or clusters, organic linkers, and their specific coordination resulting in porous crystal structures.[2,3] These advantageous features allow using MOFs as an engineering platform for targeted drug delivery systems with high loading capacity and controllable release.[4,5]

Zeolitic imidazolate frameworks (ZIFs) are a specific subclass of MOFs comprising imidazolate linkers and metal ions with structures similar to aluminosilicate zeolites.[6] In this subclass, ZIF-8 ($Zn(mim)_2$, mim = 2-methylimidazolate) has recently been extensively studied as pH-responsive drug carrier.[7–11] It possesses a porous structure with a pore diameter of 11.60 Å,[12–14] high BET surface area (1630 $m^2\ g^{-1}$)[12,14] and the ability to decompose in acidic media.[8] The latter feature has become a point of particular interest in ZIF-8 as a platform for targeted anticancer drug carriers, since the extracellular substances of tumours are known to be more acidic compared to normal tissues.[15,16] Specifically, the acidification of the tumour environment occurs due to a large amount of lactate secreted by tumour cells.[17] The modified metabolism of cancer cells results in aberrant glycolysis with the subsequent lactate secretion even in the presence of oxygen, known as the Warburg effect.[18,19]

Studies on biomedical or drug delivery systems based on ZIF-8 have often omitted details on their degradation in the real environment.[7,20–25] In several recent studies, the stability of ZIF-8 has been addressed in specific liquids such as water,[26] phosphate buffered saline (PBS),[27] serum, Dulbecco's Modified Eagle's Medium (DMEM), and other laboratory buffer systems at nearly neutral pH.[28] Taheri *et al.* have addressed the stability of ZIF-8 in bacterial culture media.[29] Alternatively, the effects of ZIF-8 degradation in acidic media with pH 5.5–6.0 have been examined using solutions with ethylenediaminetetraacetic acid (EDTA),[30] citric,[30,31] or acetic[8] acid. More often, various pH-adjusted solutions based on PBS have been used to estimate the release kinetics at neutral conditions or provide a comparison at lower pH.[7–11,32–38] The choice of PBS is usually argued by its osmolarity and ion concentrations matching the human body.

[a]*Laboratory of Solution Chemistry of Advanced Materials and Technologies, ITMO University, Lomonosova str. 9, St. Petersburg, 191002, Russian Federation. E-mail: morozov@scamt-itmo.ru*

[b]*St. Petersburg Academic University, Khlopina str. 8/3, St. Petersburg, 194021, Russian Federation*

[c]*Faculty of Chemistry and Mineralogy, Institute of Inorganic Chemistry, Leipzig University, Leipzig, D-04103, Germany*

However, a controversy of this choice may arise from the fact that the degradation of ZIF-8 is not controlled by pH solely, but may also be affected by various anions.[39] Particularly, the hydrogen phosphate anion $[HPO_4]^{2-}$ is known to affect the stability of ZIF-8,[39] and thus should be of major concern as a constituent of PBS. To date, no separate analysis has been addressed to distinguish between the extent of ZIF-8 degradation caused by protonation itself and by presence of $[HPO_4]^{2-}$ anions.

In this study, we provide a systematic analysis of ZIF-8 decomposition kinetics using common isotonic PBS (pH 7.4) and phosphate-free 0.9% saline (pH 6.3) solutions as references, while comparing with the corresponding acidic solutions with pH adjusted to 5.0 by adding lactic acid. Thus, the specific acidic environment similar to tumour extracellular secretion is properly implemented. Additionally, we address the toxicity of ZIF-8 and its decomposition products comparing their effects on the relative survival rate of human dermal fibroblasts (HDF) and human alveolar adenocarcinoma (A549) cell lines incubated in standard and phosphate-free basal media.

Materials and methods

Chemicals

2-Methylimidazole (Hmim) was purchased from Acros Organics. Zinc acetate dihydrate ($Zn(OAc)_2 \cdot 2H_2O$) was obtained from Sigma-Aldrich. L-(+)-Lactic acid (85–90% aqueous solution) was purchased from Alfa Aesar. Sterile water (H_2O, Solopharm, Russia) and 0.9% saline solution (NaCl, MosFarm, Russia) were purchased from a pharmacy store. PBS buffer was prepared by dissolving a 5 g Gibco® PBS Tablet (Thermo Fisher Scientific, USA) in 500 mL of distilled water. Cell cultures A549 and HDF were obtained from ATCC. Cell culture media DMEM (Biolot, Russia) and phosphate-free DMEM (Thermo Fisher Scientific, USA) were used for *in vitro* assays. Gentamicin additive (50 μg mL^{-1}) was used as an antibiotic.

Synthesis of ZIF-8 crystals

ZIF-8 crystals were obtained by first dissolving 293 mg $Zn(OAc)_2 \cdot 2H_2O$ in 10 mL deionised water, then adding the resultant product to a solution of 3.8 g Hmim dissolved in 20 mL deionised water. The solutions were prepared at room temperature, without stirring. The molar composition is thus equal to the following ratios: Zn/Hmim/water = 1/35/1248. After 24 h, the precipitate was separated from the colloidal dispersion by centrifugation (10 500 rpm, 20 min) and washed with deionised water three times, thus adopting the method by Jian *et al.*[40]

Material characterisation and analysis

Powder X-ray diffraction (XRD) was performed using a Rigaku SmartLab 3 diffractometer with Cu Kα radiation ($\lambda = 1.5418$ Å). Scanning electron microscopy (SEM) and energy dispersive X-ray (EDX) spectroscopy were carried out using a scanning electron microscope Supra 25 (Carl Zeiss AG) equipped with a silicon drift detector Ultim Max 100 (Oxford Instruments). Fourier-transform infrared (FTIR) spectra were recorded with a Shimadzu IRTracer-100 spectrometer using an ATR accessory with a diamond window.

Decomposition of ZIF-8 crystals

ZIF-8 crystals were immersed in deionised water, PBS buffer (pH = 7.4) and 0.9% saline solution (pH = 6.3) at a concentration of 100 μg mL^{-1}. In two additional experiments, the acidity of NaCl and PBS solutions was adjusted each to pH = 5.0 by adding the respective amount of lactic acid. For experiments on the decomposition kinetics, the probes were taken for analyses at different time periods following incubation. The decomposition rate was evaluated by monitoring the content of Hmim in the solutions using a spectrophotometer Cary 60 UV-Vis (Agilent Technologies, USA).

MTT assay

Viability of HDF and A549 cells in different media was evaluated using a standard methylthiazol tetrazolium (MTT) assay[41] adopted as follows. The cells were detached from the support with a trypsin–versene solution (1 : 1) and counted using a hemocytometer. 200 μL of cell suspension was added into a 96-well plate (Nunc, Denmark) and incubated for 72 hours (5% CO_2). In two separate experiments, ZIF-8 polycrystalline samples were added at a concentration of 0.1 mg mL^{-1} for 1 and 24 hours, respectively. An additional plate with cells solely was processed as the control batch. The assays were performed using the HDF and A549 cell lines in various combinations with two different cell media, DMEM and phosphate-free DMEM. In both cases, the cell media included additions of 5% fetal bovine serum (FBS) and 50 μg mL^{-1} gentamicin. The incubated product was tested by adding 0.2 mL of MTT (5 mg mL^{-1}) for 2 h, then the MTT-formazan product was dissolved in 0.2 mL dimethyl sulfoxide (DMSO), and the optical absorption was measured at 570 nm using a plate reader Infinite F50 (Tecan, Austria).

Results and discussion

Synthesis and characterisation of ZIF-8 crystals

Different topologies of ZIF-8 crystals[40,42–44] and related biocomposites[30,31,45–47] can be obtained by varying synthetic conditions. ZIF-8 crystals are known to form different topological polymorphs: sodalite (CSD code: VELVOY), diamondoid (CSD code: OFERUN01), ZIF-L (CSD code: IWOZOL) and katsenite (CSD code: OFERUN08), of which sodalite is the most porous.[42,43] Since porous MOF structures are typically used for encapsulation of biologically active substances,[5] we have adjusted the ratio between metal, ligand and solvent to obtain sodalite ZIF-8, following the method by Jian *et al.*[40] The crystal structure and morphology of the obtained ZIF-8 product have been examined by X-ray diffraction, SEM and EDX imaging. The results are illustrated in Fig. 1. The XRD analysis (Fig. 1a) confirms the single-phase sodalite topology (CSD code: VELVOY) with the basal spacing determined by the reflection peaks $d(110) = 12.04$ Å, $d(002) = 8.53$ Å, and $d(112) = 6.97$ Å. The SEM analysis (Fig. 1b) indicates the formation of rhombic dodecahedral crystals with a uniform size distribution (Fig. 1c) peaking

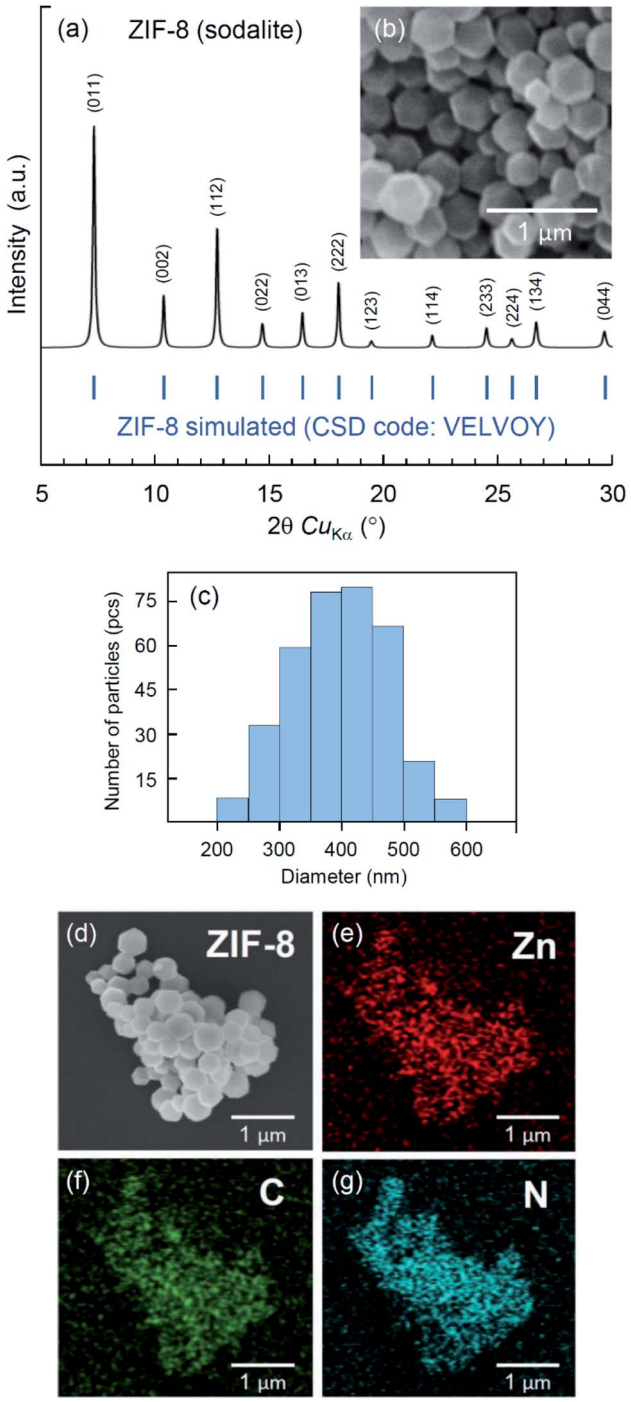

Fig. 1 (a) XRD pattern and (b) SEM image of ZIF-8 crystals; (c) crystal size distribution; (d)–(g) composition analysis of ZIF-8 microcrystals: BSE image (d) and EDX mapping of Zn (e), C (f) and N (g).

at the average diameter of 0.4 μm. The elemental mapping by the means of combined SEM imaging (Fig. 1d) and EDX spectroscopy (Fig. 1e–g) have confirmed the presence and uniform distribution of zinc (Fig. 1e), carbon (Fig. 1f) and nitrogen (Fig. 1g) throughout the crystals. The results of the material characterization are consistent with several previous studies.[48–50]

Degradation of ZIF-8 in water, PBS, and 0.9% saline solutions

In this section, we address an analysis of the relative stabilities of ZIF-8 crystals in common commercially available isotonic solutions such as PBS and aqueous NaCl. Additionally, we have made a similar test using a sample of sterile water for injections purchased from a pharmacy. The acidity of the PBS solution was adjusted manually to pH 7.4, while the acidity of a 0.9% aqueous NaCl solution and water was measured prior to the experiment to be 6.3 and 5.5, respectively. Both values are normal for ambient conditions because of carbon dioxide absorption under atmosphere pressure.[51]

Fig. 2 displays SEM images of ZIF-8 crystals taken after their incubation in PBS (pH 7.4), NaCl (pH 6.3), and water (pH 5.5) for 1 min, 30 min, 120 min and 24 hours. The results of this experiment demonstrate that the relationship between the rate of ZIF-8 degradation and the acidity of the local environment is not straightforward. Despite the lowest acidity, an immersion in PBS resulted in higher degradation compared to other media in the experiment. The crystals incubated in this buffer rapidly changed their morphology, while another crystalline phase, likely zinc phosphate, was produced. The visual manifestation of this process is mostly notable within the incubation period of 0.5 to 2 hours. In contrast, 0.9% NaCl solution with slightly higher acidity caused almost no damages to ZIF-8 crystals during a day. Finally, incubation in water that had the highest acidity in the experiment resulted in minor damages that gradually developed with time.

To shed more light on the nature of the degradation products, we analysed them by the means of EDX analysis and FTIR spectroscopy. Fig. 3 depicts an SEM image (Fig. 3a) and EDX elemental mapping of zinc (Fig. 3b), phosphorus (Fig. 3c), and oxygen (Fig. 3d) for a ZIF-8 sample subjected to treatment in PBS solution with pH 7.4 for one minute. The results suggest the

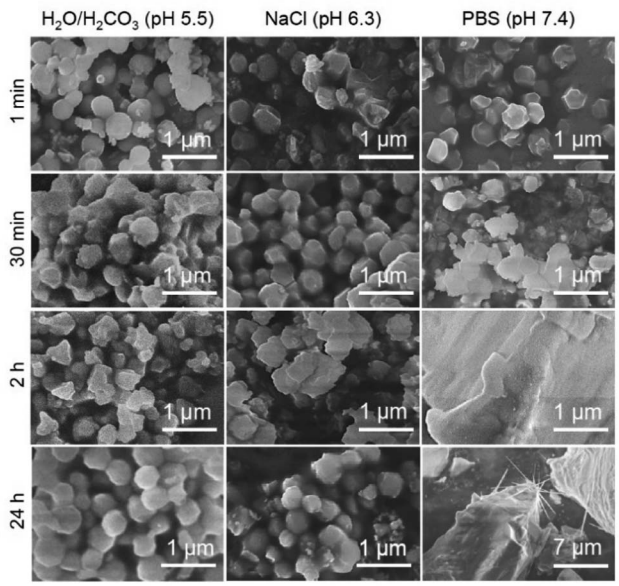

Fig. 2 SEM images of ZIF-8 crystals after incubation in H_2O, 0.9% NaCl and PBS solutions for 1 min, 30 min, 120 min and 24 hours.

interaction of ZIF-8 with PBS leads to formation of zinc phosphate crystals possessing some typical dendrite structures (Fig. 3a) that usually appear at zinc-containing reactive interfaces.[52]

Fig. 4 exhibits FTIR spectra for Hmim, ZIF-8 crystals, lactic acid, and products of ZIF-8 degradation upon immersion in 0.9% NaCl (pH 6.3), PBS (pH 7.4) and lactic acid (pH 2.8) for 24 hours. The main features of ZIF-8 and its decomposition products are well known from several previous studies.[27,53,54] In brief, the fingerprint of Hmim and ZIF-8 includes a band at 3138 cm^{-1} associated with the N–H stretching vibrations (Hmim), the aliphatic C–H stretch of imidazole manifests itself at 2929 cm^{-1}, the C=N stretching vibration is detected at 1587 cm^{-1}, the entire ring stretching appear at 1300–1460 cm^{-1}, while a band at 1145 cm^{-1} corresponds to the aromatic C–N stretching mode. The bands at 754 cm^{-1} and 679 cm^{-1} are associated with the out-of-plane ring bending vibration. A distinctive feature of ZIF-8 integrity is the Zn–N stretching vibration at 419 cm^{-1}. For lactic acid, the characteristic bands include the C=O stretching vibration at 1727 cm^{-1} (a general feature of carboxylic acids), while the bands in the region 1200–950 cm^{-1} correspond to the C–C and C–O stretching modes. The lower frequency range above 1200 cm^{-1} includes various bands corresponding to C–H, C–O and CH_3.

Degradation of ZIF-8 in strong lactic acid solution (pH 2.8) within 24 hours leaves almost no bands pertinent to ZIF-8, except the traces of the imidazole ring stretching mode. In contrast, the residual Zn–N stretching vibration at 419 cm^{-1} is observed in both samples immersed in PBS and NaCl solutions, as seen in Fig. 4, indicating an incomplete degradation of the metal complexes, which is consistent with similar observations by Velásquez-Hernández *et al.*[27] Additionally, an interaction of ZIF-8 with PBS has resulted in the appearance of a new series of bands that was proposed to be associated with phosphates:[27,55,56] the broad bands at 525 cm^{-1}, 980 cm^{-1} and 1093 cm^{-1} are attributed to the bending, antisymmetric and symmetric stretching of PO_4^{3-}, correspondingly.

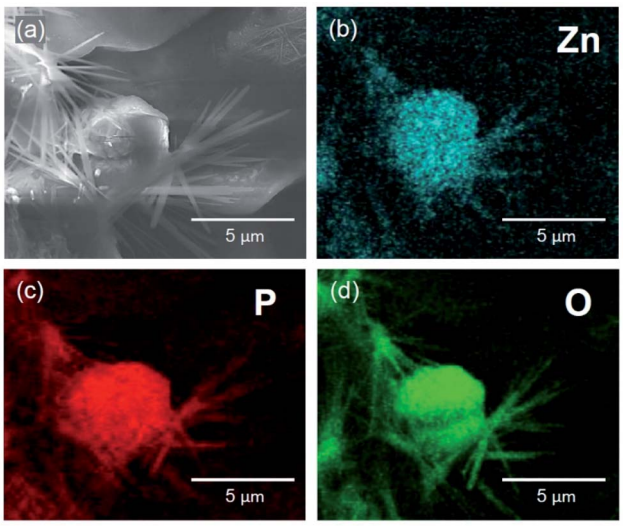

Fig. 3 SEM image (a) and EDX mapping of Zn (b), P (c), and O (d) in a sample of ZIF-8 microcrystals, treated in PBS solution with pH 7.4 for 1 minute.

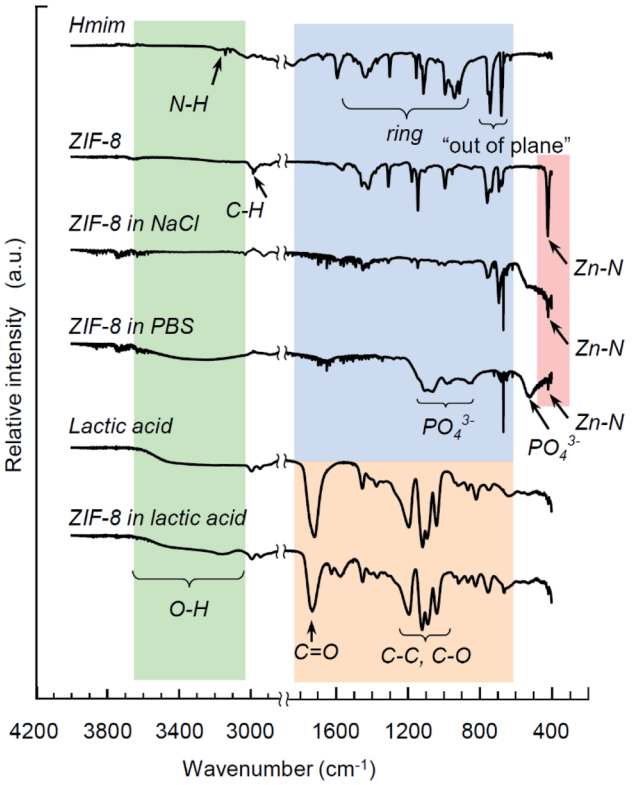

Fig. 4 FTIR spectra for Hmim, ZIF-8 crystals, lactic acid, and products of ZIF-8 degradation upon immersion in 0.9% NaCl (pH 6.3), PBS (pH 7.4) and lactic acid (pH 2.8) for 24 hours.

Degradation of ZIF-8 in PBS and NaCl solutions with lactic acid

Next, we compared the relative decomposition rates for ZIF-8 immersed in PBS and 0.9% NaCl solutions with and without presence of lactic acid. To ascertain the relevant acidity of the lactic acid for this experiment, we first evaluated the pH of various basal media, in which HDF and A549 cells had been incubated for 72 hours. As illustrated in Fig. 5, the pH of the local cell environment ranges from 6.2 for normal dermal fibroblast cells in phosphate-free DMEM to 5.3 for the pathological alveolar adenocarcinoma cells (A549) cultivated in standard DMEM. In both cases, the effect of phosphate presence on the pH of the DMEM media was minor compared to the contribution of cells secretion. Based on this evaluation and other literature data,[15,16] we have chosen a limit of pH 5.0 for the purpose of examining the kinetics, as it largely covers the ability of tumour cells to increase acidity of their local environment.

The decomposition rates of ZIF-8 crystals immersed in various media were evaluated by monitoring the light adsorption at 208 nm, which corresponds to the π–π^* transition associated with the conjugated π-bonding in the aromatic ring of 2-methylimidazole.[57,58] The result is demonstrated in Fig. 6a. The initial stage of the process is expanded in Fig. 6b. In line

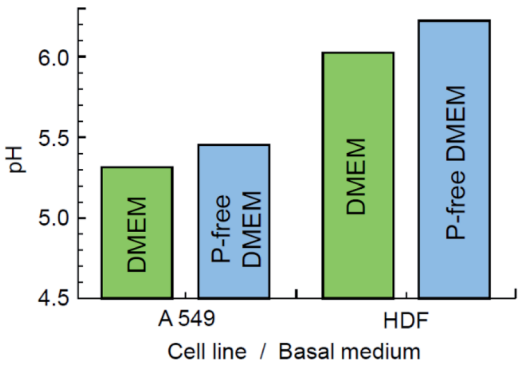

Fig. 5 Acidity of basal media with HDF and A549 cells incubated for 72 hours.

with the modern theory of crystal dissolution,[59] the observed reactions began at zero rate when conditions were far from equilibrium and then developed with a strong nonlinear decrease in the rate as equilibrium conditions were approached. In all cases, the experimentally observed slow degradation rates at the stage prior to the complete saturation have been successfully matched by the rate equations of the first order with the coefficient of determination $R^2 \geq 0.994$.

As can be seen in Fig. 6b, in the absence of phosphate anions, the degradation rate of ZIF-8 is relatively slow at the initial stage. Compared to the degradation rate in 0.9% saline solution, the presence of lactic acid in the solution enhanced the conversion in the first five hours from *ca.* 17% to *ca.* 23%, while the presence of phosphate anions without acidification resulted in *ca.* 38% conversion. In case of both lactic acid and phosphate anions being present in the media, the conversion reached *ca.* 54%. However, as seen in Fig. 6a, further degradation of ZIF-8 microcrystals in the presence of phosphate anions eventually decreased the rate. A plausible reason for this can be the formation of a protective layer by zinc phosphate on the surface of ZIF-8 polycrystalline aggregates.[27] Zinc phosphate is insoluble in water, so that the degradation of ZIF-8 in PBS may be incomplete without assistance by an acidification agent or develop with a significantly slower rate with such an assistance.

The experimentally determined kinetics (Fig. 6a) suggests a rapid degradation of ZIF-8 in PBS, reaching approximately 90% of the possible conversion, while the conversion in PBS with lactic acid reached 100%, but with a significantly lower rate. The process is schematically rationalised in Scheme 1. In accordance with the previous study of ZIF-8 degradation in PBS,[27] the possibility of complete degradation eventually depends on the size of ZIF-8 crystallites.

Thus, both phosphate anions and acidification agents are shown to be capable of affecting the decomposition kinetics of ZIF-8 crystals. At a nearly neutral pH, the presence of phosphate anions leads to a rapid degradation of ZIF-8, especially at the initial stage. This rationalizes the faster degradation of ZIF-8 crystals in PBS with pH 7.4 compared to slightly more acidic water solutions of carboxylic acid (pH 5.5) and 0.9% NaCl (pH 6.3), as illustrated in Fig. 2. In concurrence with this, an increase of the solution acidity is another competitive factor that leads to complete degradation of ZIF-8, as was exemplified by FTIR analysis (Fig. 4) for the case of ZIF-8 degradation in lactic acid with pH 2.8.

Cytotoxicity of ZIF-8 and its decomposition products

Finally, we completed our study with the characterisation of the cytotoxicity of ZIF-8 and its decomposition products. The corresponding MTT assays have been performed with normal HDF and malignant A549 cell lines incubated in standard DMEM and phosphate-free DMEM. The relative survival rates are displayed in Fig. 7. Both assays with HFD (Fig. 7a) and A549 (Fig. 7b) cells showed mild cytotoxicity as per 1 h and 24 h exposition with ZIF-8 microcrystals. Even though the presence of phosphate anions may lead to formation of insoluble zinc phosphate and cause a cytotoxic effect,[60] their vital role is apparently more essential, as their deficiency in basal media results in stronger suppression of the survival rate for both types of cells. Phosphates are ubiquitous in physiological fluids,

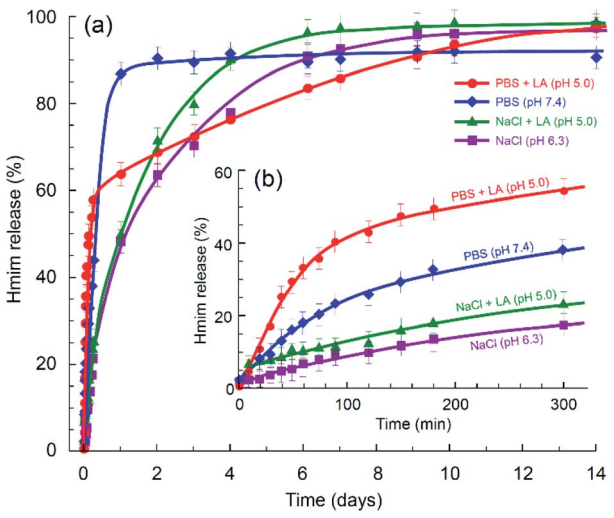

Fig. 6 Kinetics of ZIF-8 degradation in various media determined *via* amount of Hmim released: (a) long-term chart and (b) the initial stage.

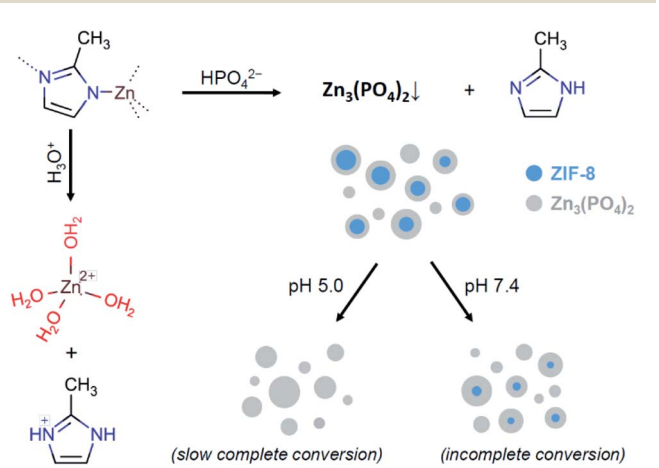

Scheme 1 Possible ways of ZIF-8 degradation.

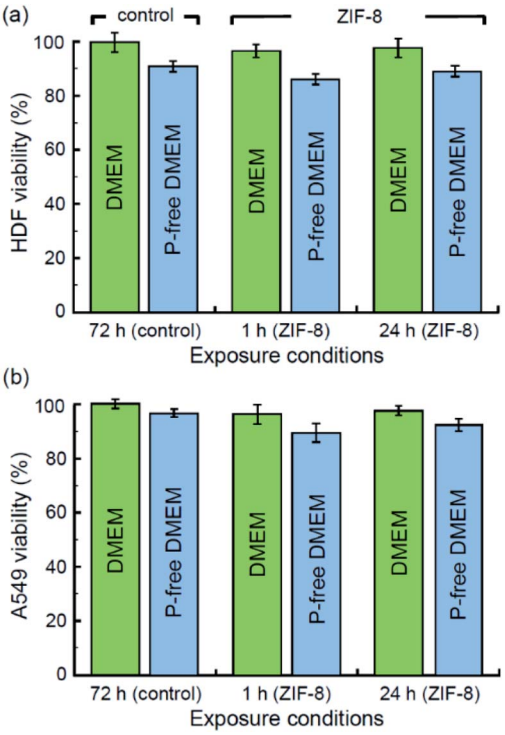

Fig. 7 Relative survival rates for (a) HDF and (b) A549 cells after incubation with ZIF-8 (1 h exposure) and its decomposition products (24 h exposure) in standard and phosphate-free basal media (DMEM).

thus formation of insoluble zinc phosphate residues upon the decomposition of ZIF-8 microcrystals seem to be the main toxicity concern of ZIF-8 application as a drug delivery platform.

Conclusion

This study has provided an insight into the role of phosphate anions and lactic acid in degrading ZIF-8 microcrystals as potential drug delivery platforms. Both agents were demonstrated to affect the rate of ZIF-8 decomposition, while the process was shown to be faster in PBS with pH 7.4 compared to an aqueous solution of 0.9% NaCl and lactic acid with pH 5.0.

As an important implication of this comparison, the pH-mediated drug release kinetics that is often reported for various drug@ZIF-8 composites and based on characterisation in PBS solutions set at different acidity (typically, pH 7.4 and 5.0) should not be misinterpreted as an exclusive effect of acidification.

Since phosphate anions are ubiquitous in physiological fluids, their combination with lactic acid is shown to moderately enhance decomposition of ZIF-8 microcrystals at the initial and relatively fast stage lasting for several hours. In contrast, at the second stage of ZIF-8 degradation, lasting for several days or weeks, the presence of phosphate anions may suppress the reaction rate by forming a protective layer of insoluble salt, likely as a result of interaction with zinc cations.

The products of ZIF-8 decomposition have demonstrated mild cytotoxicity in assays performed with normal HDF and malignant A549 cell lines within 24 hour exposure. However, the long-term toxicity of the insoluble salt product, supposedly zinc phosphate, requires further elucidation.

Conflicts of interest

The authors confirm that there are no conflicts to declare.

Acknowledgements

The work is fulfilled with the financial support from the Russian Science Foundation (Grant No. 19-19-00433). S. A. B., A. S., A. V. V. and E. H.-H. acknowledge the Erasmus+ programme for the support of students and staff mobility between ITMO University (Russia) and Leipzig University (Germany). Dr Dmitry P. Danilovich is acknowledged for his kind support with XRD and FTIR characterisation. This characterisation was conducted using facilities of the Engineering Centre at the Saint-Petersburg State Technological Institute (Technical University). The authors acknowledge Dr Alexey Mozharov (Academic University) for his assistance with EDX analysis and Prof. Evgeny A. Pidko (TU-Delft) for the useful discussion on kinetics of ZIF-8 decomposition.

References

1 Y. Sun, L. Zheng, Y. Yang, X. Qian, T. Fu, X. Li, Z. Yang, H. Yan, C. Cui and W. Tan, Metal–organic framework nanocarriers for drug delivery in biomedical applications, *Nano-Micro Lett.*, 2020, **12**, 103.

2 J. L. C. Rowsell and O. M. Yaghi, Metal–organic frameworks: a new class of porous materials, *Microporous Mesoporous Mater.*, 2004, **73**, 3–14.

3 S. M. Morozova, A. Sharsheeva, M. I. Morozov, A. V. Vinogradov and E. Hey-Hawkins, Bioresponsive metal–organic frameworks: rational design and function, *Coord. Chem. Rev.*, 2021, **431**, 213682.

4 P. Horcajada, C. Serre, M. Vallet-Regí, M. Sebban, F. Taulelle and G. Férey, Metal–organic frameworks as efficient materials for drug delivery, *Angew. Chem., Int. Ed.*, 2006, **45**, 5974–5978.

5 M. d. J. Velásquez-Hernández, M. Linares-Moreau, E. Astria, F. Carraro, M. Z. Alyami, N. M. Khashab, C. J. Sumby, C. J. Doonan and P. Falcaro, Towards applications of bioentities@MOFs in biomedicine, *Coord. Chem. Rev.*, 2021, **429**, 213651.

6 B. Chen, Z. Yang, Y. Zhu and Y. Xia, Zeolitic imidazolate framework materials: recent progress in synthesis and applications, *J. Mater. Chem. A*, 2014, **2**, 16811–16831.

7 A. Sharsheeva, V. A. Iglin, P. V. Nesterov, O. A. Kuchur, E. Garifullina, E. Hey-Hawkins, S. A. Ulasevich, E. V. Skorb, A. V. Vinogradov and M. I. Morozov, Light-controllable systems based on TiO_2-ZIF-8 composites for targeted drug release: communicating with tumour cells, *J. Mater. Chem. B*, 2019, **7**, 6810–6821.

8 C. Y. Sun, C. Qin, X. L. Wang, G. S. Yang, K. Z. Shao, Y. Q. Lan, Z. M. Su, P. Huang, C. G. Wang and E. B. Wang,

Zeolitic imidazolate framework-8 as efficient pH-sensitive drug delivery vehicle, *Dalton Trans.*, 2012, **41**, 6906–6909.

9 A. Tiwari, A. Singh, N. Garg and J. K. Randhawa, Curcumin encapsulated zeolitic imidazolate frameworks as stimuli responsive drug delivery system and their interaction with biomimetic environment, *Sci. Rep.*, 2017, **7**, 12598.

10 H. Zheng, Y. Zhang, L. Liu, W. Wan, P. Guo, A. M. Nyström and X. Zou, One-pot synthesis of metal–organic frameworks with encapsulated target molecules and their applications for controlled drug delivery, *J. Am. Chem. Soc.*, 2016, **138**, 962–968.

11 I. B. Vasconcelos, T. G. Da Silva, G. C. G. Militão, T. A. Soares, N. M. Rodrigues, M. O. Rodrigues, N. B. Da Costa, R. O. Freire and S. A. Junior, Cytotoxicity and slow release of the anti-cancer drug doxorubicin from ZIF-8, *RSC Adv.*, 2012, **2**, 9437–9442.

12 Q. Shi, Z. Chen, Z. Song, J. Li and J. Dong, Synthesis of ZIF-8 and ZIF-67 by steam-assisted conversion and an investigation of their tribological behaviors, *Angew. Chem., Int. Ed.*, 2011, **50**, 672–675.

13 R. Banerjee, High-throughput synthesis of zeolitic imidazolate frameworks and application to CO_2 capture, *Science*, 2008, **319**, 939–944.

14 K. S. Park, Z. Ni, A. P. Côté, J. Y. Choi, R. Huang, F. J. Uribe-Romo, H. K. Chae, M. O'Keeffe and O. M. Yaghi, Exceptional chemical and thermal stability of zeolitic imidazolate frameworks, *Proc. Natl. Acad. Sci. U. S. A.*, 2006, **103**, 10186–10191.

15 M. Stubbs, P. M. J. McSheehy, J. R. Griffiths and C. L. Bashford, Causes and consequences of tumour acidity and implications for treatment, *Mol. Med. Today*, 2000, **6**, 15–19.

16 K. Engin, D. B. Leeper, J. R. Cater, A. J. Thistlethwaite, L. Tupchong and J. D. Mcfarlane, Extracellular pH distribution in human tumours, *Int. J. Hyperthermia*, 1995, **11**, 211–216.

17 A. Annibaldi and C. Widmann, *Curr. Opin. Clin. Nutr. Metab. Care*, 2010, **13**, 466–470.

18 O. Warburg, On Respiratory Impairment in Cancer Cells, *Science*, 1956, **124**, 269–270.

19 O. Warburg, On the origin of cancer cells, *Science*, 1956, **123**, 309–314.

20 W. Miao, J. Wang, J. Liu and Y. Zhang, Self-cleaning and antibacterial zeolitic imidazolate framework coatings, *Adv. Mater. Interfaces*, 2018, **5**, 1800167.

21 P. Li, J. Li, X. Feng, J. Li, Y. Hao, J. Zhang, H. Wang, A. Yin, J. Zhou, X. Ma and B. Wang, Metal–organic frameworks with photocatalytic bactericidal activity for integrated air cleaning, *Nat. Commun.*, 2019, **10**, 2177.

22 S. Peng, J. Liu, Y. Qin, H. Wang, B. Cao, L. Lu and X. Yu, Metal–organic framework encapsulating hemoglobin as a high-stable and long-circulating oxygen carriers to treat hemorrhagic shock, *ACS Appl. Mater. Interfaces*, 2019, **11**, 35604–35612.

23 X. Guo, H. Yang, Q. Liu, J. Liu, R. Chen, H. Zhang, J. Yu, M. Zhang, R. Li and J. Wang, A chitosan-graphene oxide/ZIF foam with anti-biofouling ability for uranium recovery from seawater, *Chem. Eng. J.*, 2020, **382**, 122850.

24 Y. Yang, J. Zan, W. Yang, F. Qi, C. He, S. Huang, S. Peng and C. Shuai, Metal organic frameworks as a compatible reinforcement in a biopolymer bone scaffold, *Mater. Chem. Front.*, 2020, **4**, 973–984.

25 B. Tao, W. Zhao, C. Lin, Z. Yuan, Y. He, L. Lu, M. Chen, Y. Ding, Y. Yang, Z. Xia and K. Cai, Surface modification of titanium implants by ZIF-8@Levo/LBL coating for inhibition of bacterial-associated infection and enhancement of in vivo osseointegration, *Chem. Eng. J.*, 2020, **390**, 124621.

26 H. Zhang, D. Liu, Y. Yao, B. Zhang and Y. S. Lin, Stability of ZIF-8 membranes and crystalline powders in water at room temperature, *J. Membr. Sci.*, 2015, **485**, 103–111.

27 M. D. J. Velásquez-Hernández, R. Ricco, F. Carraro, F. T. Limpoco, M. Linares-Moreau, E. Leitner, H. Wiltsche, J. Rattenberger, H. Schröttner, P. Frühwirt, E. M. Stadler, G. Gescheidt, H. Amenitsch, C. J. Doonan and P. Falcaro, Degradation of ZIF-8 in phosphate buffered saline media, *CrystEngComm*, 2019, **21**, 4538–4544.

28 M. A. Luzuriaga, C. E. Benjamin, M. W. Gaertner, H. Lee, F. C. Herbert, S. Mallick and J. J. Gassensmith, ZIF-8 degrades in cell media, serum, and some—but not all—common laboratory buffers, *Supramol. Chem.*, 2019, **31**, 485–490.

29 M. Taheri, D. Ashok, T. Sen, T. G. Enge, N. K. Verma, A. Tricoli, A. Lowe, D. R. Nisbet and T. Tsuzuki, Stability of ZIF-8 nanopowders in bacterial culture media and its implication for antibacterial properties, *Chem. Eng. J.*, 2021, **413**, 127511.

30 E. Astria, M. Thonhofer, R. Ricco, W. Liang, A. Chemelli, A. Tarzia, K. Alt, C. E. Hagemeyer, J. Rattenberger, H. Schroettner, T. Wrodnigg, H. Amenitsch, D. M. Huang, C. J. Doonan and P. Falcaro, Carbohydrates@MOFs, *Mater. Horiz.*, 2019, **6**, 969–977.

31 F. Carraro, M. d. J. Velásquez-Hernández, E. Astria, W. Liang, L. Twight, C. Parise, M. Ge, Z. Huang, R. Ricco, X. Zou, L. Villanova, C. O. Kappe, C. Doonan and P. Falcaro, Phase dependent encapsulation and release profile of ZIF-based biocomposites, *Chem. Sci.*, 2020, **11**, 3397–3404.

32 J. Zhuang, C.-H. Kuo, L.-Y. Chou, D.-Y. Liu, E. Weerapana and C.-K. Tsung, Optimized metal–organic framework nanospheres for drug delivery: evaluation of small-molecule encapsulation, *ACS Nano*, 2014, **8**, 2812–2819.

33 C. Adhikari, A. Das and A. Chakraborty, Zeolitic imidazole framework (ZIF) nanospheres for easy encapsulation and controlled release of an anticancer drug doxorubicin under different external stimuli: a way toward smart drug delivery system, *Mol. Pharm.*, 2015, **12**, 3158–3166.

34 M.-T. Liang, S.-H. Wang, Y.-L. Chang, H.-I. Hsiang, H.-J. Huang, M.-H. Tsai, W.-C. Juan and S.-F. Lu, Iron oxide synthesis using a continuous hydrothermal and solvothermal system, *Ceram. Int.*, 2010, **36**, 1131–1135.

35 K. Liang, R. Ricco, C. M. Doherty, M. J. Styles, S. Bell, N. Kirby, S. Mudie, D. Haylock, A. J. Hill, C. J. Doonan and P. Falcaro, Biomimetic mineralization of metal–organic

frameworks as protective coatings for biomacromolecules, *Nat. Commun.*, 2015, **6**, 7240.

36 R. Bian, T. Wang, L. Zhang, L. Li and C. Wang, A combination of tri-modal cancer imaging and in vivo drug delivery by metal–organic framework based composite nanoparticles, *Biomater. Sci.*, 2015, **3**, 1270–1278.

37 C. Cheng, C. Li, X. Zhu, W. Han, J. Li and Y. Lv, Doxorubicin-loaded Fe_3O_4-ZIF-8 nano-composites for hepatocellular carcinoma therapy, *J. Biomater. Appl.*, 2019, **33**, 1373–1381.

38 J. Bi, Y. Lu, Y. Dong and P. Gao, Synthesis of folic acid-modified DOX@ZIF-8 nanoparticles for targeted therapy of liver cancer, *J. Nanomater.*, 2018, **2018**, 1357812.

39 H. Wang, M. Jian, Z. Qi, Y. Li, R. Liu, J. Qu and X. Zhang, Specific anion effects on the stability of zeolitic imidazolate framework-8 in aqueous solution, *Microporous Mesoporous Mater.*, 2018, **259**, 171–177.

40 M. Jian, B. Liu, R. Liu, J. Qu, H. Wang and X. Zhang, Water-based synthesis of zeolitic imidazolate framework-8 with high morphology level at room temperature, *RSC Adv.*, 2015, **5**, 48433–48441.

41 T. Mosmann, Rapid colorimetric assay for cellular growth and survival: application to proliferation and cytotoxicity, *J. Immunol. Methods*, 1983, **65**, 55–63.

42 Z. Akimbekov, A. D. Katsenis, G. P. Nagabhushana, G. Ayoub, M. Arhangelskis, A. J. Morris, T. Friščić and A. Navrotsky, Experimental and theoretical evaluation of the stability of true MOF polymorphs explains their mechanochemical interconversions, *J. Am. Chem. Soc.*, 2017, **139**, 7952–7957.

43 Y. Lo, C. H. Lam, C.-W. Chang, A.-C. Yang and D.-Y. Kang, Polymorphism/pseudopolymorphism of metal–organic frameworks composed of zinc(II) and 2-methylimidazole: synthesis, stability, and application in gas storage, *RSC Adv.*, 2016, **6**, 89148–89156.

44 R. Chen, J. Yao, Q. Gu, S. Smeets, C. Baerlocher, H. Gu, D. Zhu, W. Morris, O. M. Yaghi and H. Wang, A two-dimensional zeolitic imidazolate framework with a cushion-shaped cavity for CO_2 adsorption, *Chem. Commun.*, 2013, **49**, 9500–9502.

45 W. Liang, R. Ricco, N. K. Maddigan, R. P. Dickinson, H. Xu, Q. Li, C. J. Sumby, S. G. Bell, P. Falcaro and C. J. Doonan, Control of structure topology and spatial distribution of biomacromolecules in protein@ZIF-8 biocomposites, *Chem. Mater.*, 2018, **30**, 1069–1077.

46 N. K. Maddigan, A. Tarzia, D. M. Huang, C. J. Sumby, S. G. Bell, P. Falcaro and C. J. Doonan, Protein surface functionalisation as a general strategy for facilitating biomimetic mineralisation of ZIF-8, *Chem. Sci.*, 2018, **9**, 4217–4223.

47 S. Li, M. Dharmarwardana, R. P. Welch, C. E. Benjamin, A. M. Shamir, S. O. Nielsen and J. J. Gassensmith, Investigation of controlled growth of metal–organic frameworks on anisotropic virus particles, *ACS Appl. Mater. Interfaces*, 2018, **10**, 18161–18169.

48 L. R. de Moura Ferraz, A. É. G. A. Tabosa, D. D. S. da Silva Nascimento, A. S. Ferreira, V. de Albuquerque Wanderley Sales, J. Y. R. Silva, S. A. Júnior, L. A. Rolim, J. J. de Souza Pereira and P. J. Rolim-Neto, ZIF-8 as a Promising Drug Delivery System for Benznidazole: Development, Characterization, in Vitro Dialysis Release and Cytotoxicity, *Sci. Rep.*, 2020, **10**(1), 1–14, DOI: 10.1038/s41598-020-73848-w.

49 M. Hoop, C. F. Walde, R. Riccò, F. Mushtaq, A. Terzopoulou, X. Z. Chen, A. J. deMello, C. J. Doonan, P. Falcaro, B. J. Nelson, J. Puigmartí-Luis and S. Pané, Biocompatibility Characteristics of the Metal Organic Framework ZIF-8 for Therapeutical Applications, *Appl. Mater. Today*, 2018, **11**, 13–21, DOI: 10.1016/j.apmt.2017.12.014.

50 J. Jia, S. Zhang, K. Wen and Q. Li, Nano-Scaled Zeolitic Imidazole Framework-8 as an Efficient Carrier for the Intracellular Delivery of RNase a in Cancer Treatment, *Int. J. Nanomed.*, 2019, **14**, 9971–9981, DOI: 10.2147/ijn.s210107.

51 B. A. J. Reddi, Why is saline so acidic (and does it really matter?), *Int. J. Med. Sci.*, 2013, **10**, 747–750.

52 Y. Zuo, K. Wang, P. Pei, M. Wei, X. Liu, Y. Xiao and P. Zhang, Zinc Dendrite Growth and Inhibition Strategies, *Mater. Today Energy*, 2021, **20**, 100692, DOI: 10.1016/j.mtener.2021.100692.

53 M. J. C. Ordoñez, K. J. Balkus, J. P. Ferraris and I. H. Musselman, Molecular sieving realized with ZIF-8/Matrimid® mixed-matrix membranes, *J. Membr. Sci.*, 2010, **361**, 28–37.

54 Y. Hu, H. Kazemian, S. Rohani, Y. Huang and Y. Song, In situ high pressure study of ZIF-8 by FTIR spectroscopy, *Chem. Commun.*, 2011, **47**, 12694–12696.

55 S. H. Jung, E. Oh, D. Shim, D. H. Park, S. Cho, B. R. Lee, Y. U. Jeong, K. H. Lee and S. H. Jeong, Sonochemical synthesis of amorphous zinc phosphate nanospheres, *Bull. Korean Chem. Soc.*, 2009, **30**, 2280–2282.

56 O. Pawlig and R. Trettin, Synthesis and characterization of α-hopeite, $Zn_3(PO_4)_2 \cdot 4H_2O$, *Mater. Res. Bull.*, 1999, **34**, 1959–1966.

57 M. K. Trivedi, A. Branton, D. Trivedi, G. Nayak, G. Saikia and S. Jana, Physical and structural characterization of biofield treated imidazole derivatives, *Nat. Prod. Chem. Res.*, 2015, **3**, 187.

58 M. Motamedi, M. Ramezanzadeh, B. Ramezanzadeh and M. Mahdavian, One-pot synthesis and construction of a high performance metal–organic structured nano pigment based on nanoceria decorated cerium (III) – imidazole network (NC/CIN) for effective epoxy composite coating anti-corrosion and thermo-mechanical properties improvement, *Chem. Eng. J.*, 2020, **382**, 122820.

59 A. C. Lasaga and A. Lüttge, A model for crystal dissolution, *Eur. J. Mineral.*, 2003, **15**, 603–615.

60 W. N. Everett, C. Chern, D. Sun, R. E. McMahon, X. Zhang, W.-J. A. Chen, M. S. Hahn and H.-J. Sue, Phosphate-enhanced cytotoxicity of zinc oxide nanoparticles and agglomerates, *Toxicol. Lett.*, 2014, **225**, 177–184.